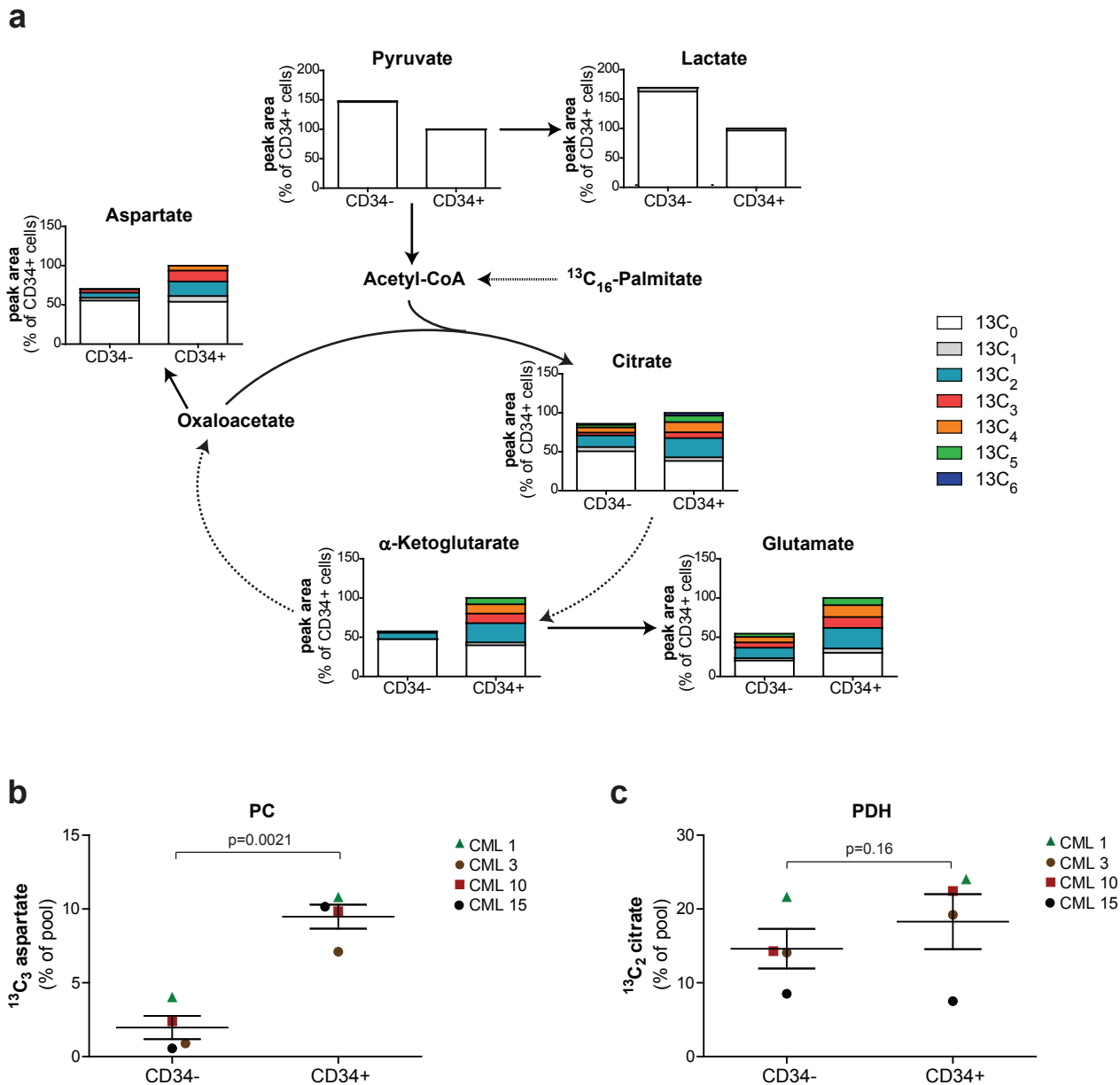


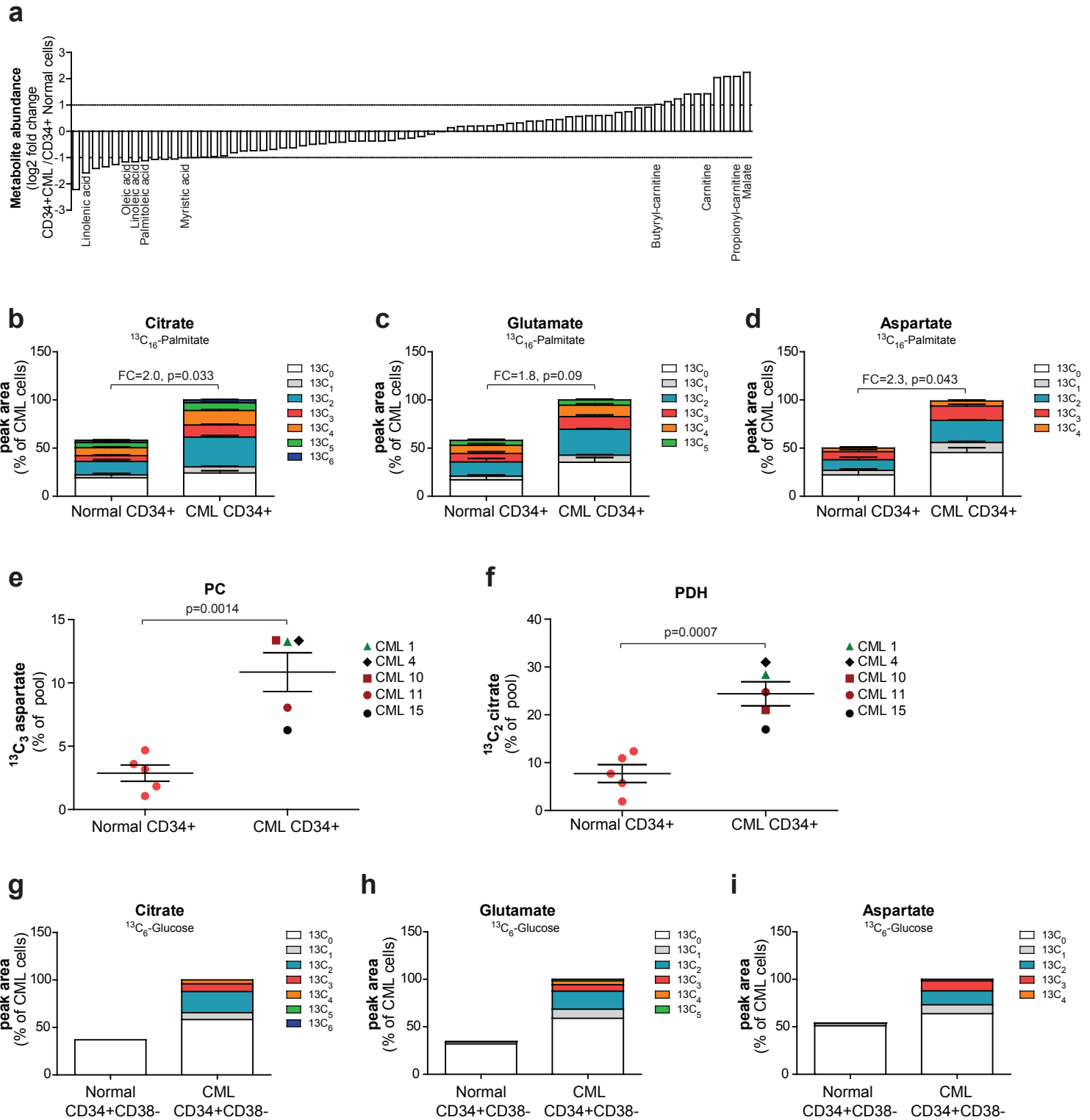
Supplementary Figure 1: Imatinib fails to eliminate LSCs.

(a) CD34 expression following *in vitro* culture of CD34⁺ CML cells with imatinib (2 μ M). (b) CD34 expression and cell death following *in vitro* culture of CD34⁺ CML cells with imatinib (2 μ M). (c) Number of colonies measured by CFC assay following 72 hours (h) drug treatment of CD34⁺ CML cells with imatinib (2 μ M). Mean \pm S.E.M. n=4 patient samples. (d) Number of colonies measured by LTC-IC assay following single drug treatment of CD34⁺ CML cells with imatinib (2 μ M). Mean \pm S.E.M. n=3 patient samples.



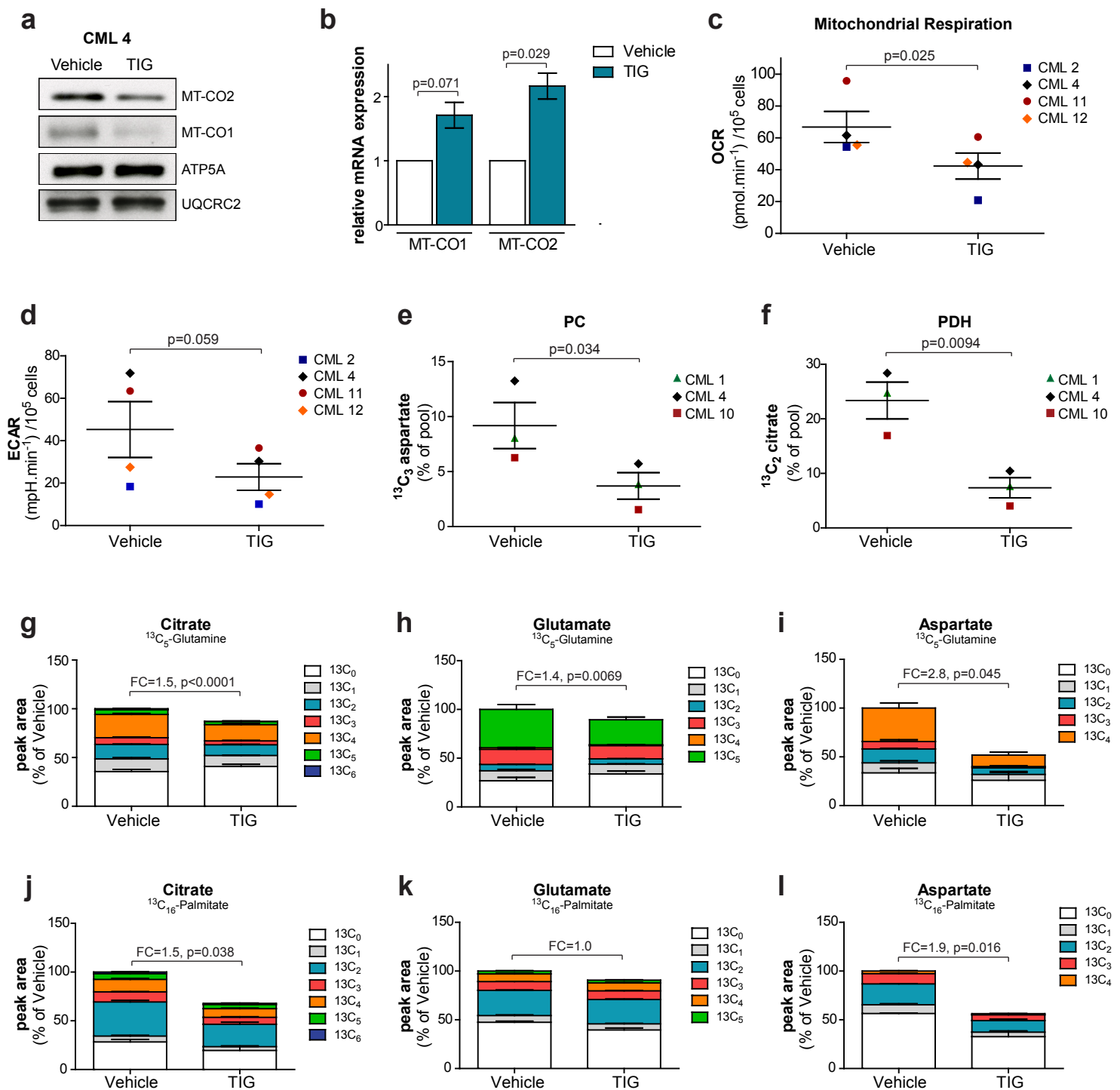
Supplementary Figure 2: Enhanced fatty acid oxidation in primitive CML cells compared to differentiated CML cells.

(a) Relative isotopologue distribution of indicated metabolites in CD34⁻ and CD34⁺ CML cells measured by LC-MS following 24 h incubation with ¹³C₁₆-labeled palmitate. n=1 patient sample. (b-c) Relative abundance of (b) ¹³C₃-aspartate and (c) ¹³C₂-citrate in CD34⁻ and CD34⁺ CML cells following 24 h incubation with ¹³C₆-labeled glucose. Mean ± S.E.M. n=4 patient samples. P-values were calculated by paired Student's t-test.



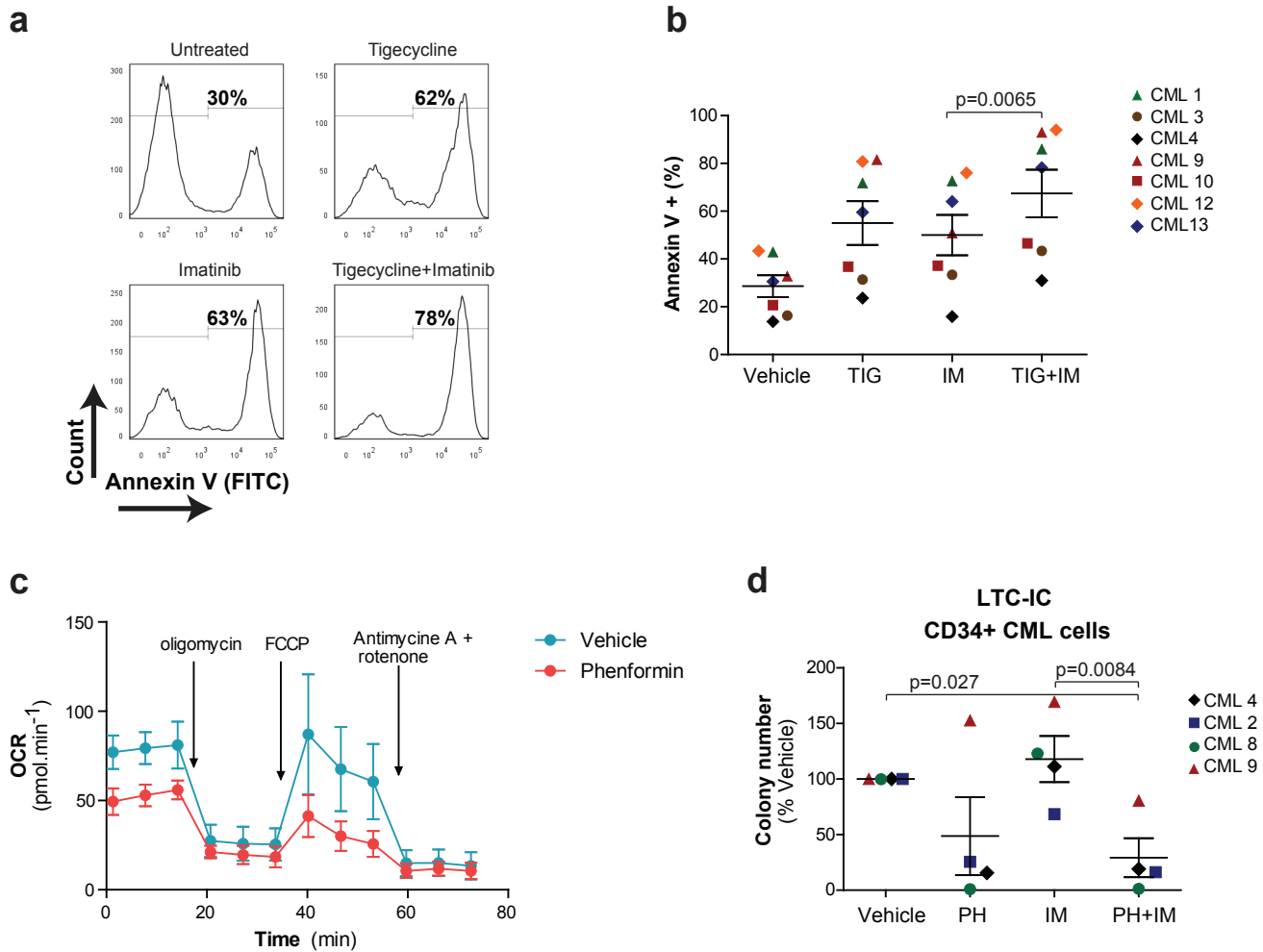
Supplementary Figure 3: Enhanced mitochondrial metabolic activity in primitive CML cells compared to normal undifferentiated hematopoietic cells.

(a) Comparative steady-state metabolomics analysis of CD34⁺ CML and CD34⁺ normal cells measured by LC-MS. n=4 patient samples. (b-d) Relative isotopologue distribution of (b) citrate, (c) glutamate and (d) aspartate in CD34⁺ CML and CD34⁺ normal cells measured by LC-MS following 24 h incubation with ¹³C₁₆-labeled palmitate. Mean ± S.E.M. n=3 patient and normal samples. FC, Fold change of palmitate-derived (¹³C_{≥2}) metabolite abundance relative to CD34⁺ normal cells. (e-f) Relative abundance (e) ¹³C₃-aspartate and (f) ¹³C₂-citrate in CD34⁺ CML and CD34⁺ normal cells following 24 h incubation with ¹³C₆-labeled glucose. n=5 patient and normal samples. (g-i) Relative isotopologue distribution of (g) citrate, (h) glutamate and (i) aspartate in CD34⁺CD38⁻ CML and CD34⁺CD38⁻ normal cells measured by LC-MS following 24 h incubation with ¹³C₆-labeled glucose. n=1 patient sample. P-values were calculated by unpaired Student's t-test.



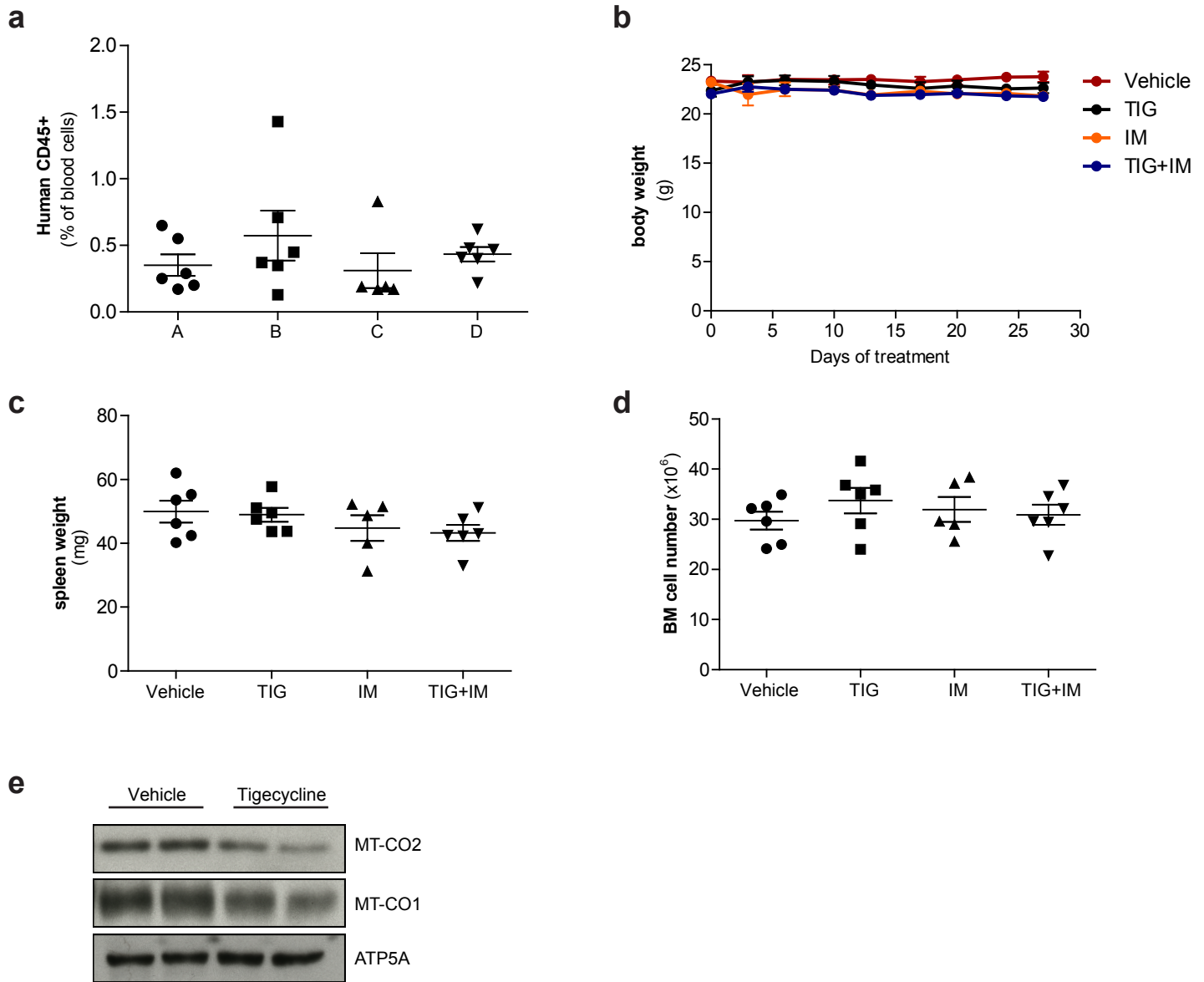
Supplementary Figure 4: Tigecycline inhibits oxidative metabolism in CD34⁺ CML cells.

(a) Protein expression in CD34⁺ CML cells following 72 h *in vitro* treatment with tigecycline (2.5 μM). n=1 patient sample (b) mRNA levels following 72 h *in vitro* treatment with tigecycline (2.5 μM). n=3 patient samples. (c) Basal mitochondrial OCR in CD34⁺ CML cells following treatment with tigecycline (2.5 μM). n=4 patient samples. (d) Basal Extracellular Acidification Rate (ECAR) in CD34⁺ CML cells following treatment with tigecycline (2.5 μM). n=4 patient samples. (e-f) Relative abundance of (e) ¹³C₃-aspartate and (f) ¹³C₂-citrate in CD34⁺ CML cells following 24 h incubation with ¹³C₆-labeled glucose in presence or absence of tigecycline (2.5 μM). n=3 patient samples. (g-i) Relative isotopologue distribution of (g) citrate, (h) glutamate and (i) aspartate in CD34⁺ CML cells measured by LC-MS following 24 h incubation with ¹³C₅-labeled glutamine in presence or absence of tigecycline (2.5 μM). n=3 patient samples. (j-l) Relative isotopologue distribution of (j) citrate, (k) glutamate and (l) aspartate in CD34⁺ CML cells measured by LC-MS following 24 h incubation with ¹³C₁₆-labeled palmitate in presence or absence of tigecycline (2.5 μM). n=3 patient samples. P-values were calculated by paired Student's t-test. All data are represented as Mean ± S.E.M.



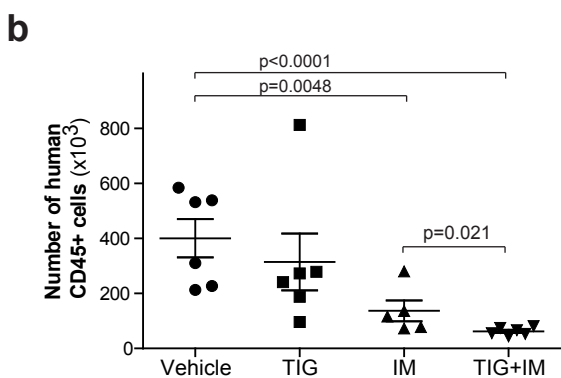
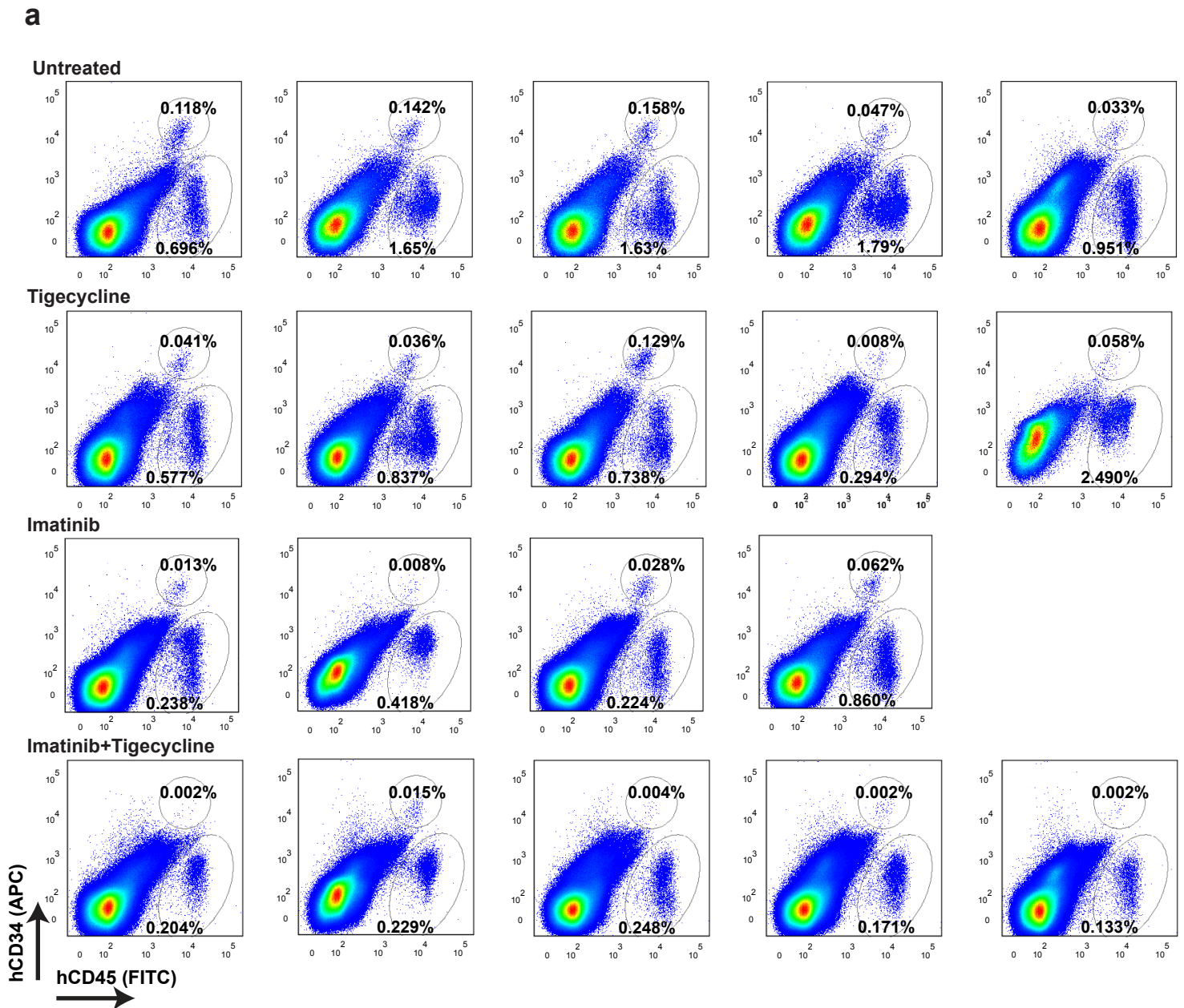
Supplementary Figure 5: Inhibition of mitochondrial activity targets primitive CML cells.

(a) Representative flow cytometry histograms and (b) percentage of Annexin V positive cells after 72 h treatment with tigecycline (2.5 μ M), imatinib (2 μ M) and combination (2.5 μ M + 2 μ M) in CD34⁺ CML cells. Mean \pm S.E.M. n=7 patient samples. (c) Representative respirometry output in CD34⁺ CML following 24 h treatment with phenformin (10 μ M). Mean \pm S.D. n=1 patient sample. (d) Number of colonies measured by LTC-IC assay in CD34⁺ CML cells. Mean \pm S.E.M. n=4 patient samples. P-values were calculated by paired Student's t-test.

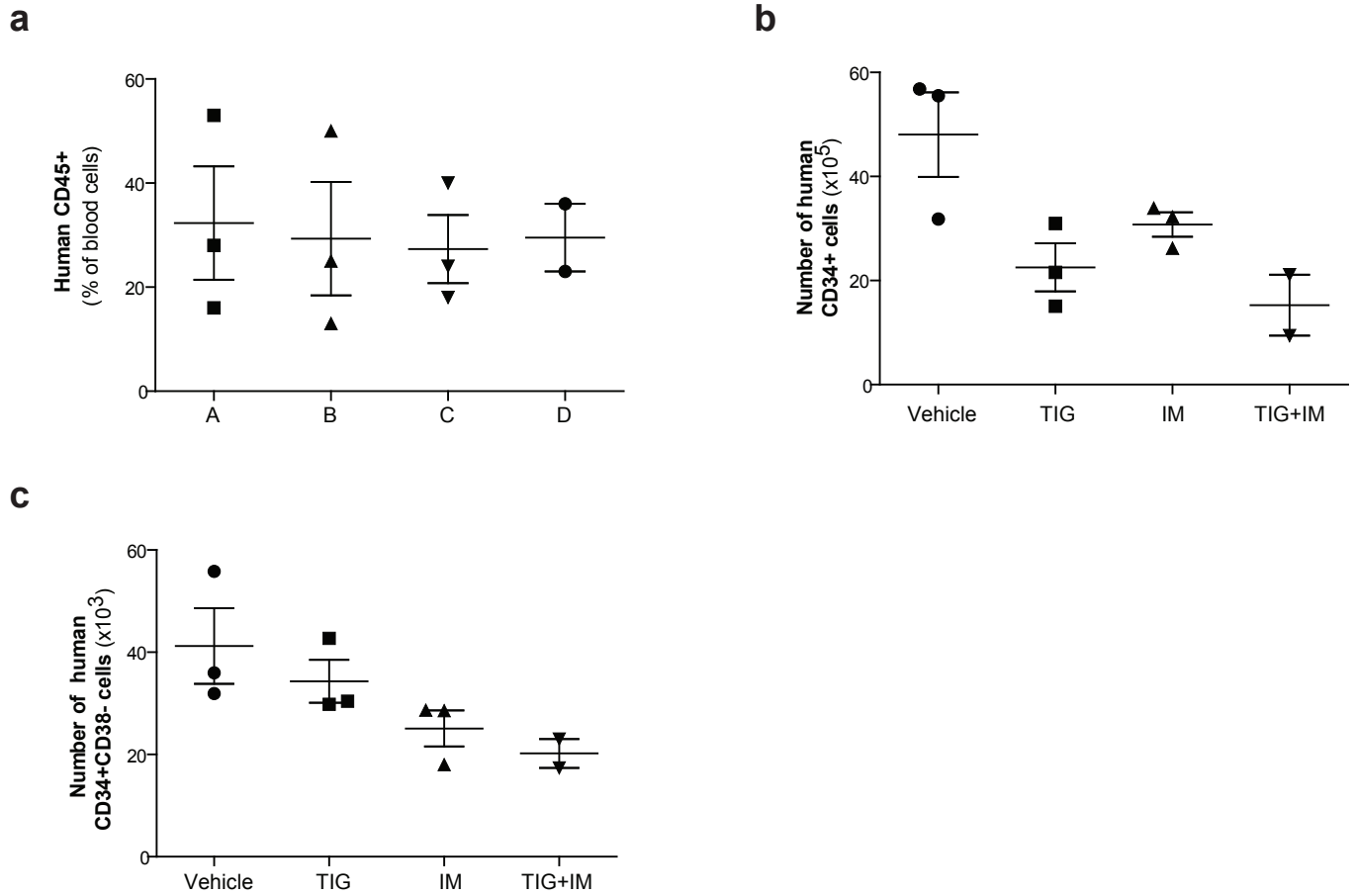


Supplementary Figure 6: *In vivo* tigecycline and/or imatinib treatment is not toxic towards normal murine cells.

(a) Percentage of human CD45⁺ cells in the blood of immuno-compromised mice prior to drug treatment. Group A, B, C and D were later on treated with Vehicle, TIG, IM and TIG+IM respectively. (b) Change in mice body weights upon drug treatment. (c) Spleen weight and (d) bone marrow cellularity of mice engrafted with CD34⁺ CML cells after 4 weeks of treatment with the indicated drugs. (e) Protein expression in FACS-sorted CD34⁺ CML cells following 4 weeks *in vivo* drug treatment. Mean \pm S.E.M.



Supplementary Figure 7: The combination of imatinib and tigecycline targets CML stem-cells *in vivo*. Mice were transplanted with CD34⁺ CML cells and analysis of human cell engraftment was performed following 4 weeks of drug treatment. **(a)** Percentage of human CD45⁺ and human CD34⁺ cells from total bone marrow cells. **(b)** Number of human CD45⁺ cells engrafted in the bone marrow of immuno-compromised mice. Mean ± S.E.M. P-values were calculated by unpaired Student's t-test on logarithmically transformed variables to meet the assumption of normality.



Supplementary Figure 8: Tigecycline marginally affects normal HSCs *in vivo*.

(a) The pre-treatment engraftment levels of cord blood cells in immuno-compromised mice were assessed by monitoring the percentage of human CD45⁺ circulating leukocytes. Group A, B, C and D were later on treated with Vehicle, TIG, IM and TIG+IM respectively. (b-c) Number of (b) human CD34⁺ and (c) human CD34⁺CD38⁻ cord blood cells engrafted in the bone marrow following *in vivo* drug treatment. n_≥2 mice per treatment arm. TIG, tigecycline; IM, imatinib.